Millimeter-Wave CMOS Digital Controlled Artificial Dielectric Differential Mode Transmission Lines for Reconfigurable ICs

Tim LaRocca, Sai-Wang Tam, Daquan Huang, Qun Gu, Eran Socher, William Hant, and Frank Chang

Department of Electrical Engineering, University of California, Los Angeles, CA, 90095, USA

***Abstract* — Digital control of the effective dielectric constant of a differential mode transmission line is shown up to 60GHz in standard CMOS technology. The effective dielectric constant is shown to increase from 5 to over 50 for the fixed artificial dielectric case. The digital controlled artificial dielectric transmission line (DiCAD) uses MOS switches to dynamically control the phase. DiCAD achieves 50% of the physically available tuning range with effective dielectric constants varying between 7 and 28. Measured results favorably agree with full-wave electromagnetic simulations.**

***Index Terms* — Coplanar Transmission Lines, Slow Wave Structures, Digital Control, Permittivity, Phase Shifters.**

I. Introduction

Cognitive, or software-defined, radio has only seriously been considered within the last couple of years, while millimeter-wave radio systems have largely been confined to small volume military and science based markets. This paper introduces a technique to electronically reconfigure the effective dielectric constant of the basic element in high-frequency design: the transmission line. This ability to alter the effective dielectric constant potentially opens the door for re-configurable, millimeter-wave circuitry using a low-cost silicon process. To date, millimeter-wave commercial markets have never fully developed, primarily due to material and manufacturing costs - a consequence of the use of expensive high-performance, but less available, III-V based semiconductor technology. With the advent of deep submicron CMOS transistors with measured f_t above 140GHz [1], academia and industry are proving the viability of low-cost, high-yield silicon CMOS as a millimeter-wave integrated circuit technology [2]-[3]. This work on electronically reconfigurable transmission lines may become an enabling technology for the future development of millimeter wave cognitive radio, and other multi-band, multi-mode (variable bandwidth) applications, such as IEEE 802.15, chip-to-chip communication, and network-on-chip RF-interconnect [4].

Artificial dielectric has long been known within the antenna community for reducing the size of lenses [5], but only recently has this concept been introduced to CMOS within a VCO [6] and as a single-ended coplanar waveguide [7]. In both cases, the artificial dielectric transmission line is in a non-reconfigurable form. The standard practice in antennas is to insert a matrix of electrically small, conductive elements within a lens material. When an electromagnetic wave is incident upon the lens, the conductive elements act as small dipoles which create a polarization vector in the same direction as the E-field. This electrical moment effectively increases the effective dielectric constant to ε' where [8]

$$\mathbf{D} = \varepsilon_0\mathbf{E} + \mathbf{P} = \varepsilon'\mathbf{E}. \quad (1)$$

In a standard, digital CMOS process with multiple (typically greater than six) metal interconnect layers, a similar effect can be replicated by inserting floating metal strips underneath a planar transmission line such as coplanar strip as shown in Fig. 1a [9]. These strips can dramatically increase the effective dielectric constant to greater than 50 even though the dielectric constant of silicon dioxide and of silicon is roughly 4.1 and 11.9 respectively. This work exploits the artificial dielectric effect by minimizing H in Fig. 1a, and shows how the ε_{eff} changes with respect to the physical parameters of the differential transmission line. This is important as millimeter-wave circuit design moves toward differential designs and away from standard, single-ended architectures.

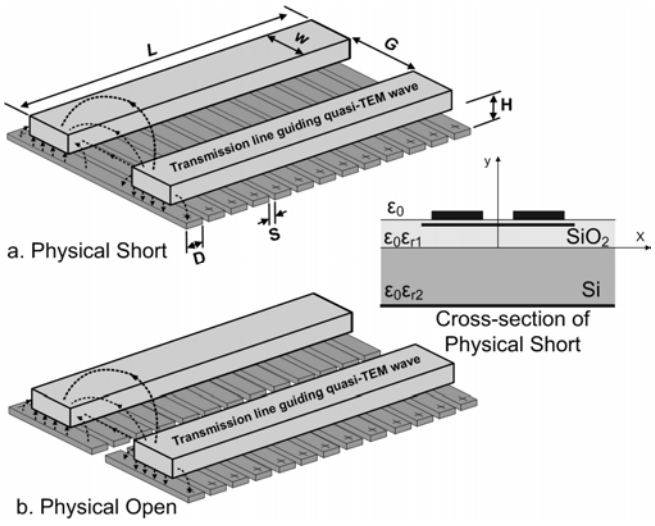

Fig. 1. Differential transmission lines with (a) artificial dielectric strips (Physical Short) and (b) cut strips (Physical Open).

Digital control of an artificial dielectric (DiCAD) transmission line is accomplished by means of a switch network situated midway along the artificial dielectric strip as shown in Fig. 2. By turning the switches between "on"

and "off", we can control the boost in dielectric constant between the maximum (all switches on) and the minimum (all switches off). Now, the artificial dielectric differential transmission line concept becomes much more powerful than simply a method to reduce size and substrate noise [6,8,9]. The DiCAD transmission line can be used as the basis for re-configurable designs such as tunable band-select filters and amplifiers, phase shifters, single-chip multi-rate modulators (BPSK, 8PSK, 16QAM), wide tuning range VCOs, and more for future millimeter-wave applications.

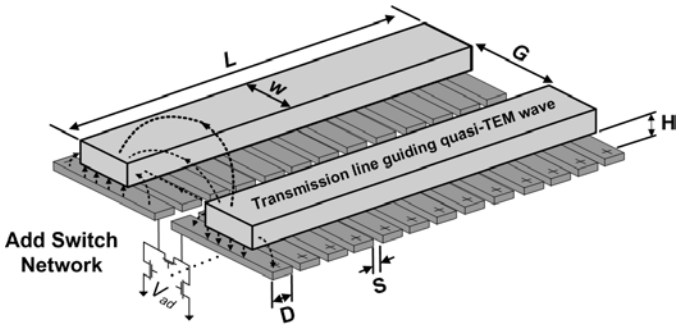

Fig. 2. Digital controlled artificial dielectric (DiCAD) differential transmission line with NMOS switch network.

II. Fixed Artificial Dielectric

A. Definitions

The relationship between the physical parameters of the transmission line and the effective dielectric constant are obtained for *physical short* and *physical open* structures as shown in Fig.1. The difference between the two is that the artificial dielectric strip in the physical open structure is physically cut, Fig. 1b, to prevent the effective dielectric boost. From measurements of the S parameters of these two structures (and subsequent conversions to ABCD and Z-parameters), we calculate the propagation constant β

$$\beta = imag(\gamma) = imag\left(\frac{1}{\ell}\cosh^{-1}\left(\frac{A+D}{2}\right)\right). \quad (2)$$

Effective dielectric constant, ε_{eff}, is obtained from

$$\varepsilon_{eff} = \left(\frac{\beta c}{2\pi f}\right)^2. \quad (3)$$

Boost factor, κ, can be estimated from

$$\kappa = \left(\frac{\phi_{S21\_ON}}{\phi_{S21\_OFF}}\right)^2 = \left(\frac{\beta_{ON}\ell}{\beta_{OFF}\ell}\right)^2 = \left(\frac{\varepsilon_{eff\_ON}}{\varepsilon_{eff\_OFF}}\right). \quad (4)$$

Note that the parameters in (2)-(4) are based on measured S-parameters after they have been de-embedded from the 50 Ohm wafer probe measurement system.

Each test requires two structures to be probed. Structures include the same input and output feed interconnect which is removed during the calibration process for simplified de-embedding. Tests are performed using a two-port de-embedding method in [10], as well as a custom designed, on-chip artificial dielectric based TRL calibration to create reference planes for accurate transmission phase data. Fig. 3 is a picture of a 150μm long physical short test structure. The feed interconnects are removed up to port 1 and port 2.

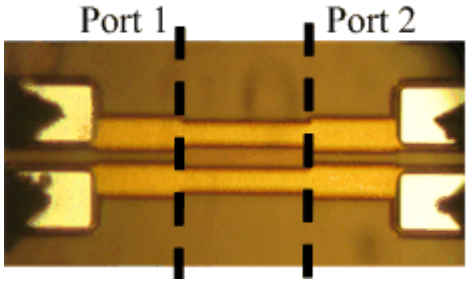

Fig. 3. Example layout of artificial dielectric transmission line with reference planes shown as dashed lines.

Measured results as shown in Fig. 4 illustrate a dramatic change in S21 phase between a physical short versus a physical open. At 60 GHz the phase increases from -35.6deg to -96.5deg. This corresponds to an effective dielectric constant change from 10.8 to 79.9 and a boost factor of 7.4.

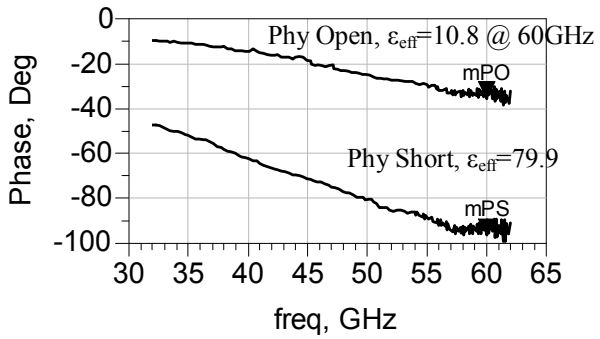

Fig. 4. Measured phase shift of physical short and open.

B. Physical Parameter Relationship

Figs. 5-8 show the relationships between the effective dielectric constant and the physical parameters of the differential transmission line: W, G, H, and S (see Fig.1). The baseline dimensions for the figures are the following: W=24μm, G=20μm, H=0.55μm, D=3μm and S=1μm (IBM

0.18µm CMOS technology). All of the data is extracted at 60GHz, and compared with electromagnetic simulation results using Sonnet Software©. Finally, the trends can be explained by the equivalent inductance and capacitance of the transmission line since (neglecting loss)

$$\upsilon = \frac{c}{\sqrt{\varepsilon_{eff}}} = \frac{1}{\sqrt{L_{eq}C_{eq}}}. \qquad (5)$$

In Fig. 5, the linear increase in the effective dielectric constant of the physical short with width (W) occurs because of the increase in area of the parallel plate capacitance between the transmission line and the artificial dielectric strips.

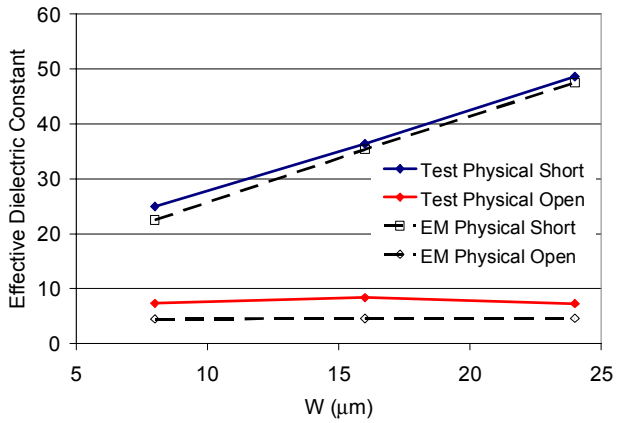

Fig. 5. Effective dielectric constant versus width (W) variation.

As the gap, G, increases, the L_{eq} for both physical open and short lines increases. For the physical open, C_{eq} decreases with increasing G, so that the $L_{eq}C_{eq}$ product remains roughly the same. For the physical short, the C_{eq} is dominated by the parallel-plate capacitance which does not change. Hence, the $L_{eq}C_{eq}$ product increases, and the effective dielectric constant increases with G in Fig. 6.

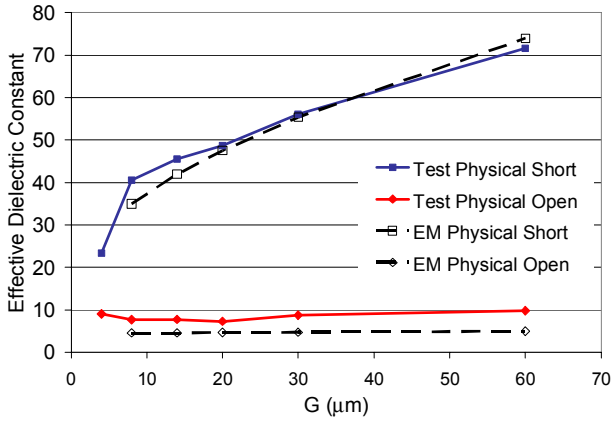

Fig. 6. Effective dielectric constant versus gap (G) variation.

The inverse relationship between the effective dielectric constant and height H, shown in Fig. 7 is similar to the change in parallel plate capacitance with distance between plates.

As shown in Fig. 8, the spacing between strips should be kept to a minimum to maximize the boost effect as well shield the structure from the lossy, silicon substrate. This is due to the decrease in unit cell capacitance, or rather the decrease in the ratio of length with an artificial dielectric strip to the length without the strip.

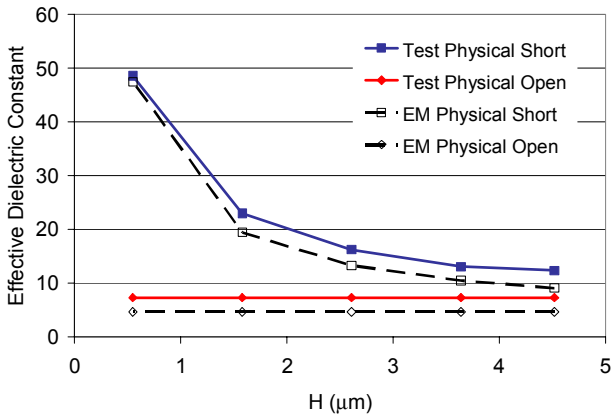

Fig. 7. Effective dielectric constant versus height (H) variation.

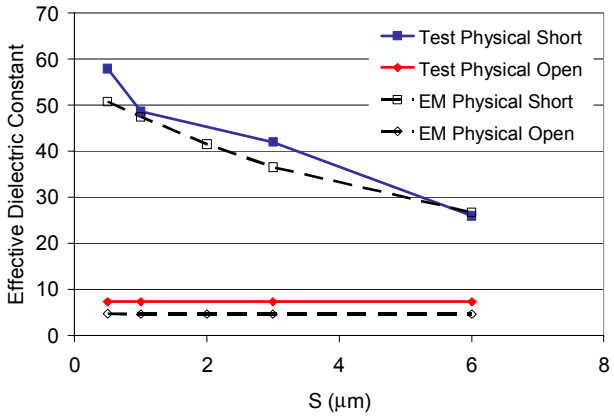

Fig. 8. Effective dielectric constant versus spacing (S).

VI. Digital Controlled Artificial Dielectric (DiCAD)

In this section we introduce the DiCAD concept, which is the significant contribution of this work. As mentioned in the introduction, a switch network is placed midway along the artificial dielectric strip. The switch network consists of three NMOS devices in a π-configuration to allow a DC ground path to the center switch source and drain to counter the effect of gate leakage on the gate-to-source potential. This switch network both turns "on" or "off" the effective

boost of the strip, and can thus be used to digitally control the millimeter-wave transmission properties of the differential transmission line.

Using an IBM 90nm standard CMOS digital process technology with a 1.2V supply voltage, a DiCAD differential line with 34 strips was measured. The artificial dielectric strip width and spacing are each 3µm, and the length of the differential transmission line is 200µm with a width and gap of 24µm and 20µm, respectively. All the switches are tied to a single control for this phase of the project, and the measurement verifies the range. The width and length of the shunt NMOS are 6µm and 0.1µm, while the center NMOS is 6µm and 0.3µm respectively. The phase change is 20deg which is 50% of the physically available range as shown in Fig. 9. The parasitic capacitance and resistance of the NMOS prevent a full 100% re-capture, 50% is a good ratio that will allow significant flexibility in reconfigurable integrated circuit design. The control voltage is swept from 0V to 1.2V to show the effectiveness of the switch network as shown in Fig. 9. It should be noted the loss of the DiCAD line is approximately -4dB/mm when off, while it increases beyond -14dB/mm with the switches on. Thus, there is a tradeoff between re-configurability and loss.

The effective dielectric constant of the DiCAD differential transmission line exhibits a boost factor of 4, and ε_{eff} increases from approximately 7 to 28 as shown in Fig.10, and correlates with simulation. This is a novel capability of electrical (non-mechanical) digital control of ε_{eff} for a transmission line.

VII. Conclusion

This paper is the first to demonstrate the concept of a *digital controlled artificial dielectric (DiCAD)* millimeter-wave differential transmission line using a standard digital CMOS process. This unique element can be used as the basis for reconfigurable integrated circuit design for low cost, multi-band and multi-rate millimeter-wave systems

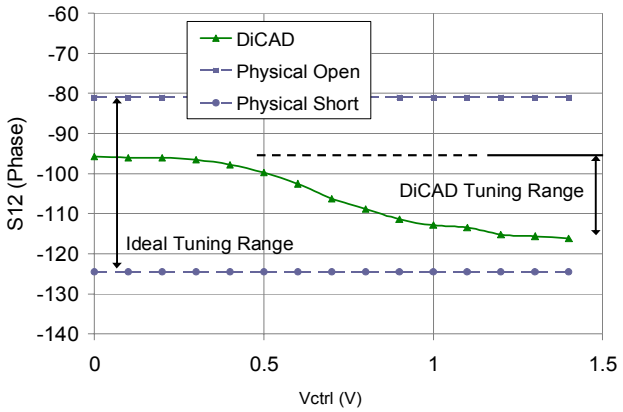

Fig. 9. Phase shift versus switch control voltage.

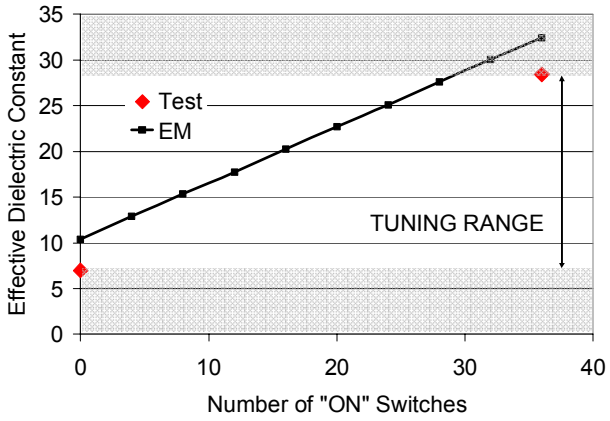

Fig.10. Effective dielectric constant versus number of switches.

Acknowledgement

Authors thank the contractual support of US DARPA/SPAWAR and the support of Raytheon Foundation.

References

[1] RF and A/MS Technologies for Wireless Technologies, ITRS Roadmap. Available: http://www.itrs.net/.

[2] D. Huang, et. al, "A 60GHz CMOS Differential Receiver Front-End Using On-Chip Transformer for 1.2 Volt Operation with Enhanced Gain and Linearity," *2006 VLSI Circuit Symposium*, pp. 144-145, 2006.

[3] B. Heydari, et. al., "Millimeter-Wave Devices and Circuit Blocks up to 104GHz in 90nm CMOS", *IEEE J. Solid-State Circuits,* vol. 42, no. 12, pp. 2893-2903, December 2007.

[4] M.F. Chang, et. al., "CMP Network-on-Chip Overlaid With Multi-Band RF Interconnect," *IEEE High Performance Computer Architecture*, February 2008

[5] W.E. Kock, "Metallic Delay Lenses," *Bell Syst. Tech. J.*, vol. 27, pp.58-82, 1948.

[6] D. Huang, "A 60GHz CMOS VCO Using On-Chip Resonator with Embedded Artificial Dielectric for Size, Loss and Noise Reduction," *ISSCC,* February 2006.

[7] T.S. Cheung, et. al., "On-Chip Interconnect for mm-Wave Applications Using an All-Copper Technology and Wavelength Reduction," *ISSCC,* February 2003.

[8] R.E. Collin, *Field Theory of Guided Waves 2nd Edition,* New Jersey: IEEE Press, 1991.

[9] T.S. Cheung, et. al., "Shielded Passive Devices for Silicon-Based Monolithic Microwave and Millimeter-Wave Integrated Circuits," *IEEE J. Solid-State Circuits,* vol. 41, no. 5, May 2006.

[10] T.E. Kolding, "On-Wafer Calibration Techniques for Giga-Hertz CMOS Measurements," *Proc. IEEE 1999 Int. Conf. on Microelectronic Test Structures,* vol. 12, March 1999.